Geomorphology 125 (2011) 517–529

Contents lists available at ScienceDirect

Geomorphology

journal homepage: www.elsevier.com/locate/geomorph

Glacis geometry as a geomorphic marker of recent tectonics: The Guadix–Baza basin (South Spain)

F.J. García-Tortosa [a,*], P. Alfaro [b], C. Sanz de Galdeano [c], J. Galindo-Zaldívar [c,d]

[a] *Departamento de Geología, Facultad de Ciencias, Universidad de Jaén, Campus Las Lagunillas, 23071 Jaén, Spain*
[b] *Departamento de Ciencias de la Tierra y del Medio Ambiente, Facultad de Ciencias, Universidad de Alicante, 03080 Alicante, Spain*
[c] *Instituto Andaluz de Ciencias de la Tierra (CSIC-Universidad de Granada), Facultad de Ciencias, Univ. Granada, 18071 Granada, Spain*
[d] *Departamento de Geodinámica, Facultad de Ciencias, Universidad de Granada, 18071 Granada, Spain*

ARTICLE INFO

Article history:
Received 11 March 2010
Received in revised form 5 October 2010
Accepted 18 October 2010
Available online 26 October 2010

Keywords:
Tectonic geomorphology
Glacis
Pediment
Active normal fault
Active folds
Guadix–Baza basin
Betic Cordillera

ABSTRACT

The Guadix–Baza basin occupies 4000 km^2, and constitutes the largest intramontane basin of the Betic Cordillera (Southern Spain). It has a well preserved geomorphic surface, a glacis, which started to be eroded when the basin conditions changed from endorheic to exorheic. Taking into account its large preserved surface area (more than 1200 km^2) and its pre-deformational geometry, this geomorphic surface is a useful marker of recent deformation. Combining geological and geomorphological data and high resolution DEM, topographic profiles of the glacis have been produced to estimate vertical displacements caused by active compression and extension structures. These structures have produced relative vertical displacements of up to 100 m from the late middle Pleistocene to the present. Assuming an age for the glacis of between 205 and 600 ka, it has been possible to estimate long-term minimum and maximum vertical rates of the activity of normal faults and folds using this geomorphic surface as a marker. Vertical slip rates range from 0.07 to 0.49 mm/year for the main active normal faults and vertical folding rates range from 0.05 to 0.17 mm/year for several active folds. These long-term vertical slip and folding rates are in accordance with other values previously estimated in other sectors of the Betic Cordillera. When present, detailed geomorphic study of recent glacis is an excellent tool for evaluating active tectonics over large regions.

1. Introduction

The recognition and quantification of recent tectonic activity through the study of landforms is one of the principal objectives of Tectonic Geomorphology (Mayer, 1986; Keller and Pinter, 1996; Yeats et al., 1997; Schumm et al., 2000; Burbank and Anderson, 2001). Traditionally, in tectonic geomorphology studies, geomorphic indices from geological, geomorphological and topographic maps, aerial photographs and field work, can be compared between different regions. However, these indices must be analysed according to other external factors such as climate, lithology, and orientation of stratification or fractures (Keller and Pinter, 1996; Ramírez, 1999; Silva et al., 2003; and many others).

As well as geomorphic indices, there are linear and planar geomorphic markers that allow qualitative and quantitative recognition and evaluation of tectonic activity of a region. Horizontal or gently dipping tectonic markers are especially useful for calculating vertical displacements caused by folds and faults. According to Burbank and Anderson (2001), the best geomorphic markers for studying recent tectonic deformation are readily recognizable landforms displaying the following three characteristics: (1) known pre-deformational geometry, (2) recent known age, and (3) high preservation potential with respect to the time-scale of the tectonic processes to be analysed.

Planar surfaces such as fluvial terraces, alluvial fans or marine terraces have been used widely as geomorphic markers to define tectonic deformation (e.g. Goy and Zazo, 1986; Goy et al., 1993; Zazo et al., 2000; Silva, 1994; Hetzel et al., 2002; Silva et al., 2003; Hetzel et al., 2004b; Filocamo et al., 2009). Nevertheless, other planar geomorphic markers such as glacis and/or pediments have been less used as geomorphic markers (Hetzel et al., 2004a; Gutiérrez et al., 2008; Hall et al., 2008) due to their eroded nature, which makes dating difficult.

In the Guadix–Baza basin there is a highly-exposed Pleistocene glacis which is preserved across a large surface area (more than 1200 km^2). The main aim of this research was to test the suitability of this geomorphic glacis surface for calculating long-term tectonic rates in large areas, such as the Guadix Baza basin. A morphometric analysis of recent deformation was performed using GIS, with a high resolution DEM, and a combined geological and geomorphological field study. The GIS data have enabled: (1) obtaining a three-dimensional detailed mapping of a large surface area, (2) identifying

---

* Corresponding author. Tel.: +34 953 212772.
E-mail address: gtortosa@ujaen.es (F.J. García-Tortosa).

0169-555X/$ – see front matter © 2010 Elsevier B.V. All rights reserved.
doi:10.1016/j.geomorph.2010.10.021

the larger deformed areas, and (3) calculating long-term tectonic rates, even in areas characterized by low deformation.

The combined use of Pliocene and Pleistocene stratigraphic markers and this geomorphic marker has provided new evidence of: (1) coexistence of active extension and compression structures in the central Betic Cordillera, some of them not previously described, and (2) new data about the more recent evolution of the basin, from the middle Pleistocene to the present, where no regional stratigraphic markers exist. Finally, assuming the age of the glacis from recently published chronostratigraphic data of the basin, new vertical slip and folding rates of the region have been estimated.

2. Geological context

The Guadix–Baza basin is an intramontane basin located in the central Betic Cordillera (Fig. 1). Its mean height above sea level is 800 m, reaching 600 m in several valley bottoms. It is bounded by Mesozoic carbonate and marl rocks belonging to the External Zone of the Betic Cordillera to the northwest, and by Triassic and Paleozoic metamorphic rocks of the Internal Zone to the southeast. The sedimentary fill is made up of upper Miocene marine rocks and Pliocene/Pleistocene fluvial and lacustrine rocks. The marine basin became continental between the end of the Miocene and the beginning of the Pliocene (Vera, 1970). Regional uplift of the central Betic Cordillera separated this basin from the Mediterranean Sea through the "Almanzora corridor" and from the Atlantic Ocean across the Guadalquivir basin. Relative uplift of the surrounding relief created differential subsidence allowing continental sedimentation in the basin during the Pliocene and a large part of the Pleistocene. At this time a great lake formed in the eastern half of the basin (Vera, 1970; Peña, 1985; Gibert, 2006; Gibert et al. 2007). In the western portion of the basin, fluvial environments developed (Vera, 1970; Viseras, 1991).

From a geomorphological point of view, during the Pleistocene an extensive glacis developed in the whole basin (Fig. 1). This surface remained active until the basin became exorheic in the middle Pleistocene, when a tributary of the Guadalquivir river captured the drainage of the basin towards the Atlantic Ocean.

From a tectonic point of view, from the late Miocene to the present, this basin has been mainly subject to N–S to NNW–SSE compression combined with an orthogonal extension (Sanz de Galdeano, 1990; Galindo-Zaldívar et al., 2003). In this regional stress field, the basement and the sedimentary cover of the Guadix–Baza basin are affected by coeval extension and compression structures of diverse age and importance (Fig. 1). Some of these structures became inactive during the late Miocene or Pliocene. But others faults, such as the Baza Fault, have an associated seismic activity (Alfaro et al., 2008). In addition, several Pleistocene seismites have been described in the basin although it is not possible to know their causative fault (Gibert et al., 2005; Alfaro et al., 2010).

The more recent basin structures deforming the Upper Pliocene and Pleistocene markers are analysed below.

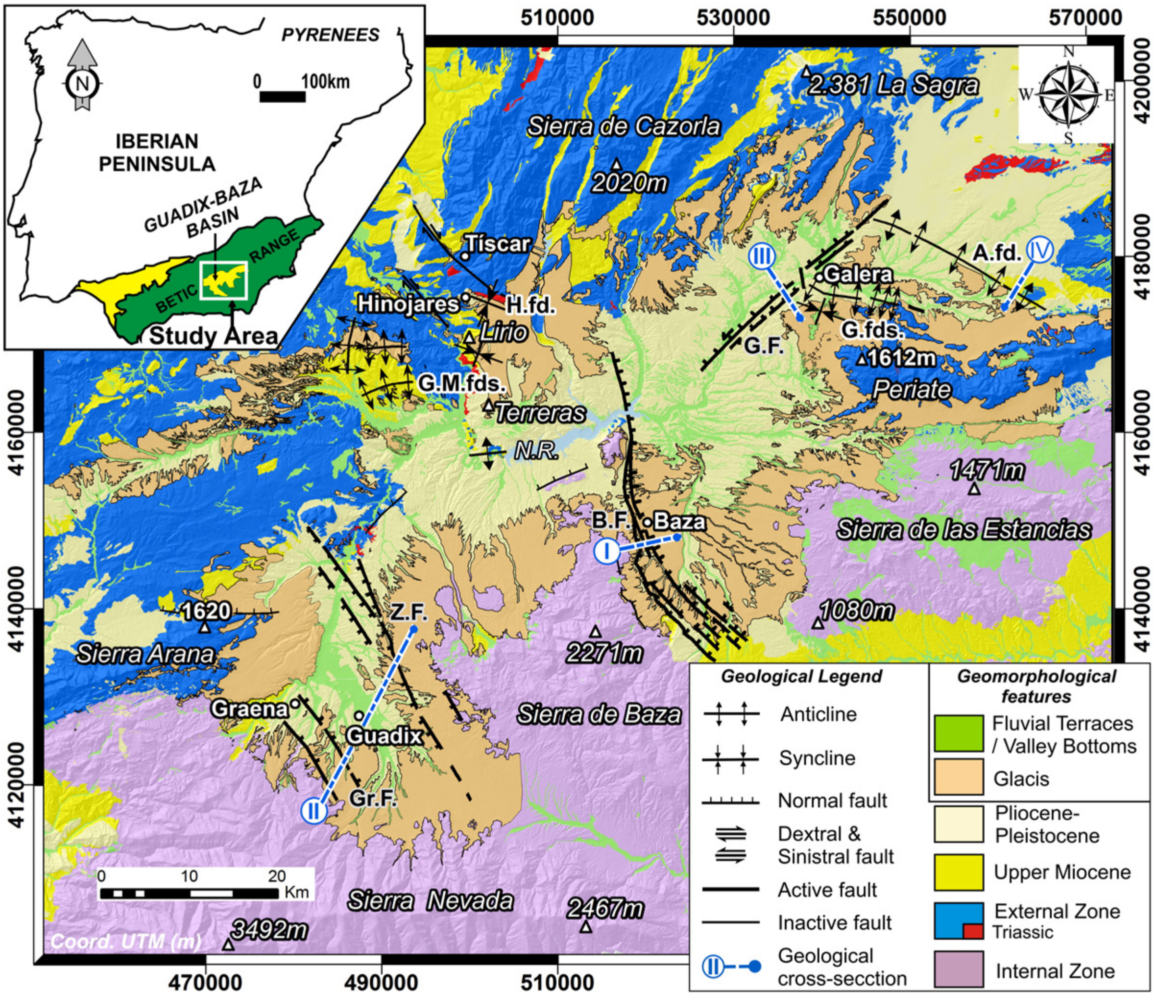

Fig. 1. Location of the study area in the central Betic Cordillera (South Spain) and general geological map of the Guadix–Baza Basin, showing the main geological structures. B.F.: Baza Fault; G.F.: Galera Fault; Gr.F.: Graena Fault; Z.F.: Zamborino Fault; A.fd.: Alfahuara fold; G.fd.: Galera folds; G.M.fds.: Guadiana Menor folds; H.fd.: Hinojares fold. Location of the geological cross-sections of Figs. 2 (I), 3 (II), 4 (III) and 5 (IV) are also included. N.R.: Negratín Reservoir.

2.1. Recent faults

The most important recent faults in the basin are normal faults with a NNW–SSE to N–S strike: the Baza Fault, the Zamborino Fault and the Graena Fault. In addition, the normal left-lateral Galera Fault is prominent (Fig. 1).

The Baza Fault is a normal fault, 37 km long, which has a NW–SE to N–S strike, and dip ranging between 45° and 65° ENE (Figs. 1, 2). The fault zone has several roughly parallel splays which are more numerous at the southern end (García-Tortosa et al., 2008) whereas towards the north they converge. The fault throw, produced from the late Miocene to the Present, is about 2 km (Alfaro et al., 2008). Its movement divided the basin into two sub-basins, the Guadix to the west and Baza to the east, determining the distribution of lacustrine sediments in the basin. Recent fault activity has developed a 30 km-long mountain front with a deduced vertical slip rate of between 0.12 and 0.33 mm/year (Alfaro et al., 2008). This fault was responsible for the 1531 Baza earthquake (Alfaro et al., 2008), with an assigned intensity of VIII-IX MMI (Martínez Solares and Mezcua, 2002) and an estimated mb magnitude of 5.1 (López-Casado et al., 2000).

The Zamborino Fault (Fig. 1) is a NNW–SSE normal fault, nearly 30 km long, dipping on average 45° to the SW. It has a wide fault zone similar to the Baza Fault, with several splays that produce topographic escarpments (Fig. 3). The Zamborino and Baza normal faults generate a horst that leaves the mid-western sector of the basin elevated.

The Graena Fault (Fig. 1) is constituted by several NW–SE normal faults developed at the boundary between the basement rocks of Sierra Nevada and the Guadix–Baza basin. These SE-dipping splays, nearly 10 km long, produce vertical displacements of metres to tens of metres in Pleistocene fluvial rocks (Fig. 3). Several minor earthquakes have been located in the graben of the Zamborino–Graena normal faults, such as the earthquakes in 1994 with a $m_{bLg}=3.2$ and 3.3 (Peláez et al., 2007).

The Galera Fault is a N50°E left-lateral normal fault, 23 km in length (Fig. 1). It has a 1.5 km-wide fault zone with several parallel splays dipping northwestwards between 40° and 60°, although local vertical dips have also been observed (Fig. 4). Deformation along the Galera Fault produces a NE–SW elongated asymmetric anticline at the surface. This fault was responsible for the 1964 Galera earthquake, with an assigned intensity of VIII and a $m_{bLg}=4.8$.

2.2. Growth folds

Recent folds of the upper Miocene to middle Pleistocene sedimentary infill are mainly orientated E–W to WNW–ESE, although associated N–S folds have also been observed. The most noticeable

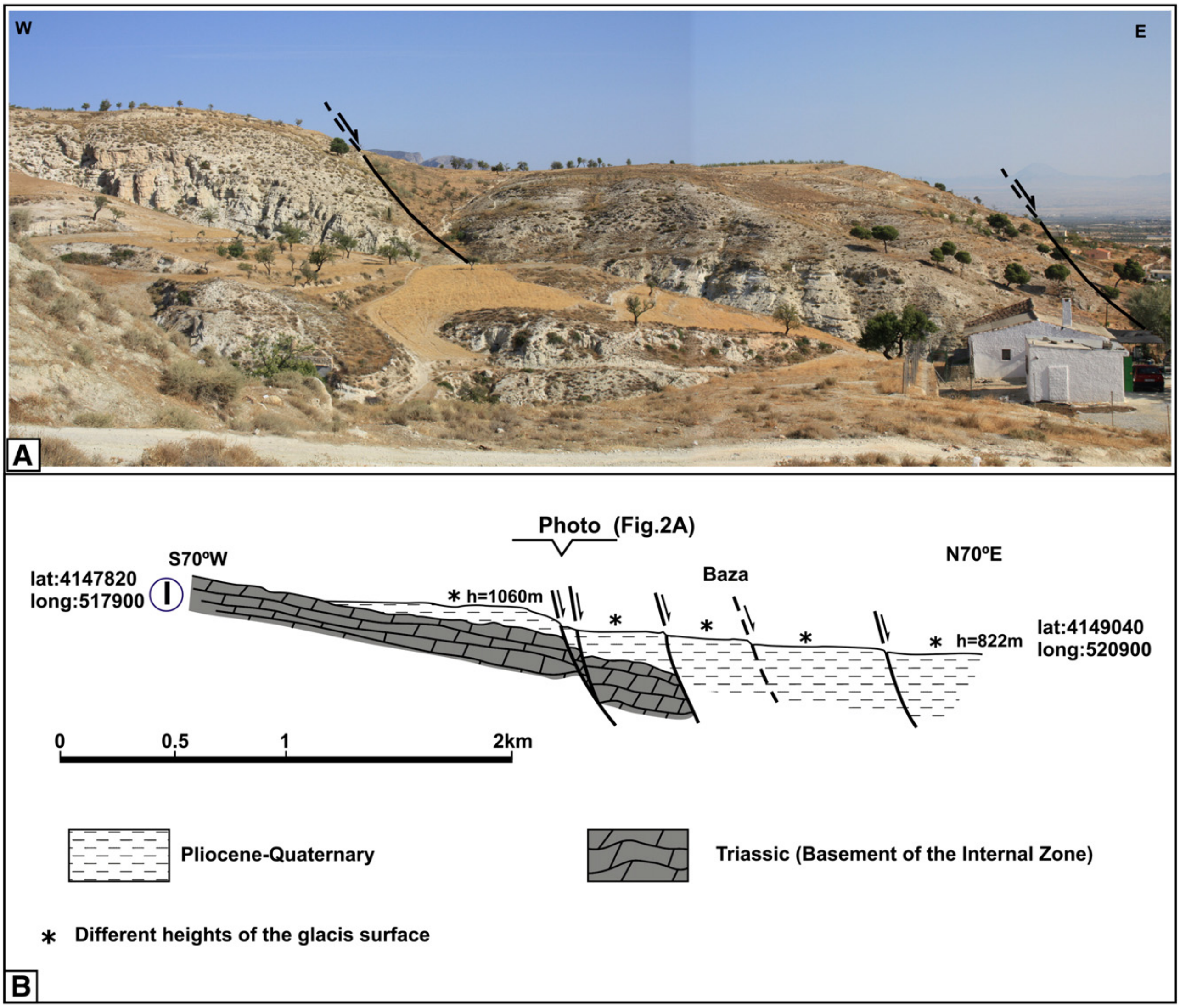

Fig. 2. A. Panoramic view of two splays of the Baza Fault zone next to the Baza town. B. Geological cross-section of the Baza Fault zone showing the glacis at different altitudes (modified from García-Tortosa et al., 2008). Their locations are indicated in Fig. 1.

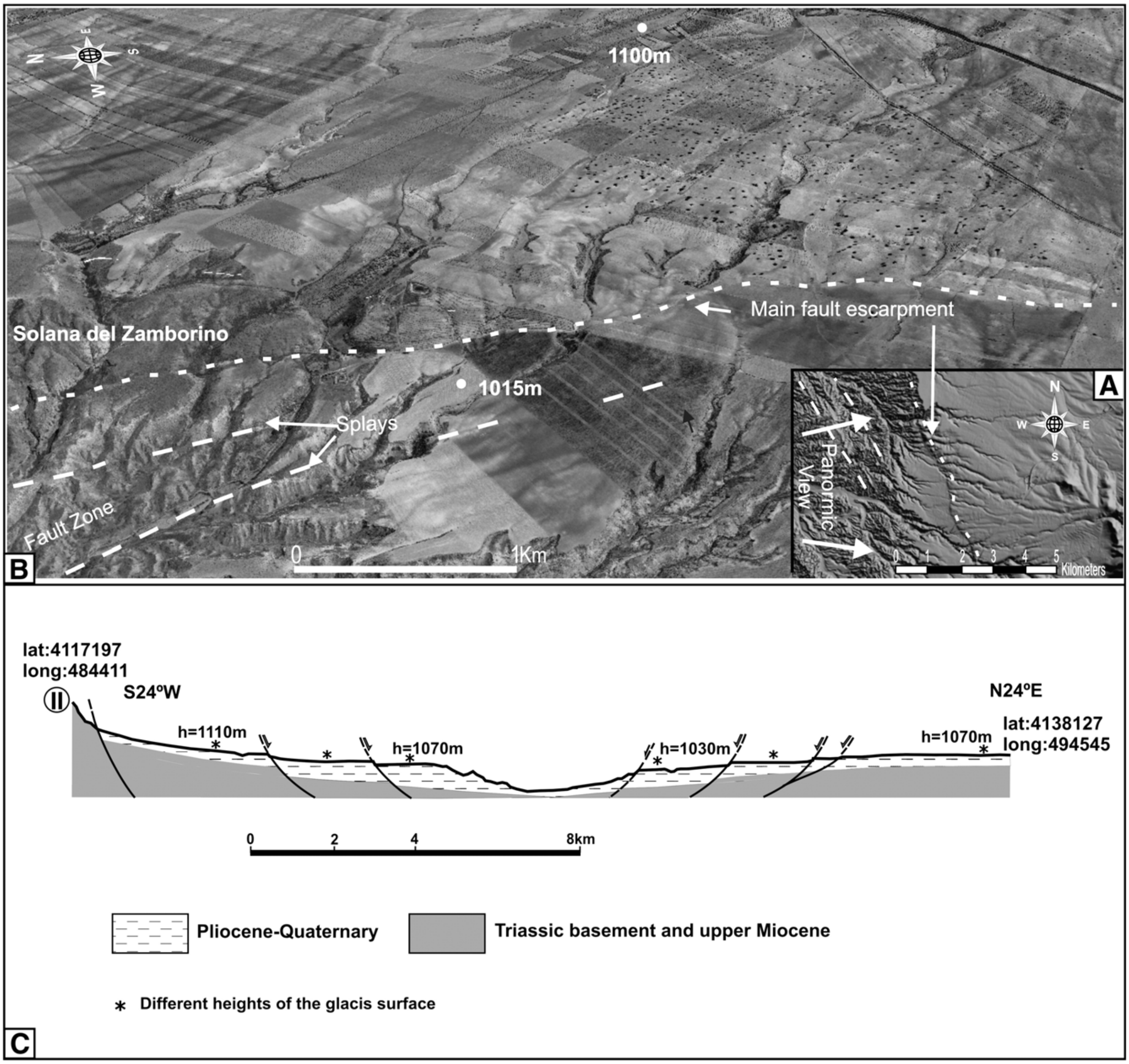

Fig. 3. A. Orthogonal view of the Zamborino Fault, indicating the panoramic view of Fig. 5B. B. DEM showing a panoramic view of the main escarpment of the Zamborino Fault which produces a step topography. C. Geological cross-section of the Zamborino–Graena graben. Their locations are indicated in Fig. 1.

active folds of the basin are located in two sectors (Fig. 1): (1) Alfahuara anticline and the Galera folds in the Baza sub-basin, and (2) Guadiana Menor folds in the Guadix sub-basin.

In the Baza sub-basin, the Alfahuara anticline produces a N120°E-elongated structural relief along 20 km. This is a growth fold developed in upper Miocene, Pliocene and Pleistocene rocks. In the northern limb, dips decrease from nearly 90° of upper Miocene sandstones to 5° of Pleistocene conglomerates, sands and clays. In the southern limb, dips of Pliocene and Pleistocene beds vary from 20° to 5°. Several travertines and discontinuous small faults could be related to a blind fault (Fig. 5). This anticline corresponds to the NE border of the Guadix–Baza basin. To the south of the Alfahuara anticline and to the East of the Galera Fault the area is characterized by folds of hectometric wavelength (Fig. 6). These folds, named the Galera folds, have a main N100–110°E strike. Several orthogonal gentle to open N10–15°E folds are also located in this area. These orthogonal axes are probably related to basement heterogeneities.

Another folded region is located in the NW sector of the basin, around the Guadiana Menor River. This sector is characterized by E–W folds (Negratín and Media Fanega folds), and NNE–SSW folds (Terreras and Lirio folds). The N85°E Negratín anticline, previously described by López-Garrido and Vera (1974) and Estévez et al. (1978), is a 5 km elongated structure deforming upper Miocene–Pleistocene rocks. In the Media Fanega folded area, located approximately 10 km northwest of the Negratín anticline, there are two main E–W anticlines separated by an open syncline deforming upper Miocene–Pleistocene rocks. The Terreras and Lirio folds also deform Pleistocene rocks and the glacis (Figs. 7, 8). Triassic evaporites and clays crop out along their hinge zones. To the north is the Hinojares fold, a WNW-growth syncline formed in Pleistocene rocks.

3. The glacis of the Guadix–Baza basin as a geomorphic marker

Throughout the endorheic geological history of the basin, a widely extended glacis developed. Relief produced by tectonic structures described earlier (particularly anticlines and fault foot walls) was eroded, creating this well-defined geomorphological surface. Only occasional relief formed by basement rocks existed in the basin area.

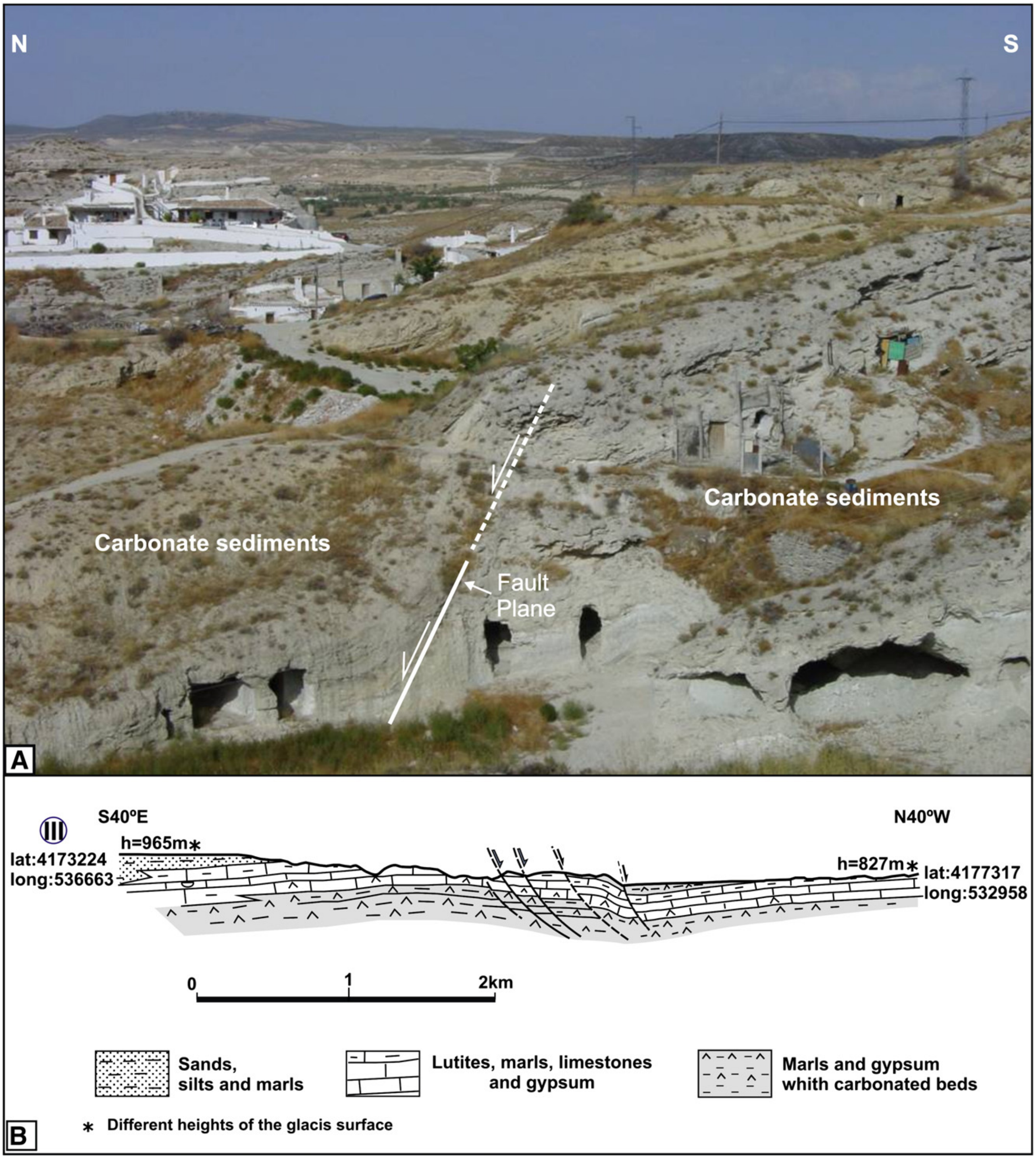

Fig. 4. A. Panoramic view of a splay of the Galera Fault in the upper part of this town. B. Geological cross-section of the Galera Fault zone showing the vertical glacis displacement. Their locations are indicated in Fig. 1.

For this reason, the Guadix–Baza glacis is, at present, eroding sediments of different ages.

The glacis is a concave surface with a gentle slope from the margins towards the centre. It slopes toward the edges, where it reaches an average altitude of 1050 m asl and exhibits dip slopes of between 6° and 3°, decreasing toward the central zones of the basin where the surface has been extensively eroded. In the central sectors of the basin, the preserved glacis has an average altitude of between 850 and 925 m, while the observed slope exhibits values as low as 2°. In the middle Pleistocene, when the Guadix–Baza basin was captured by the Guadalquivir River, erosion dominated over sedimentation. The glacis was progressively eroded, and a badland landscape developed, which is still active at present. In spite of that, the glacis represents the most characteristic geomorphological feature of the Guadix–Baza basin, which enables reconstruction of its original morphology (García-Tortosa et al., 2008; Pérez-Peña et al., 2009).

The glacis paleosurface represents the last trace of the endorheic period of the basin. The first dating of the endhoreic–exorheic transition was based on the stratigraphic position of the archaeological–paleontological site of Solana del Zamborino, located nearly at the top of the endorheic succession of the basin. Botella et al. (1985) assigned an age of 100 ka due to its Acheulean lithic industry. Several

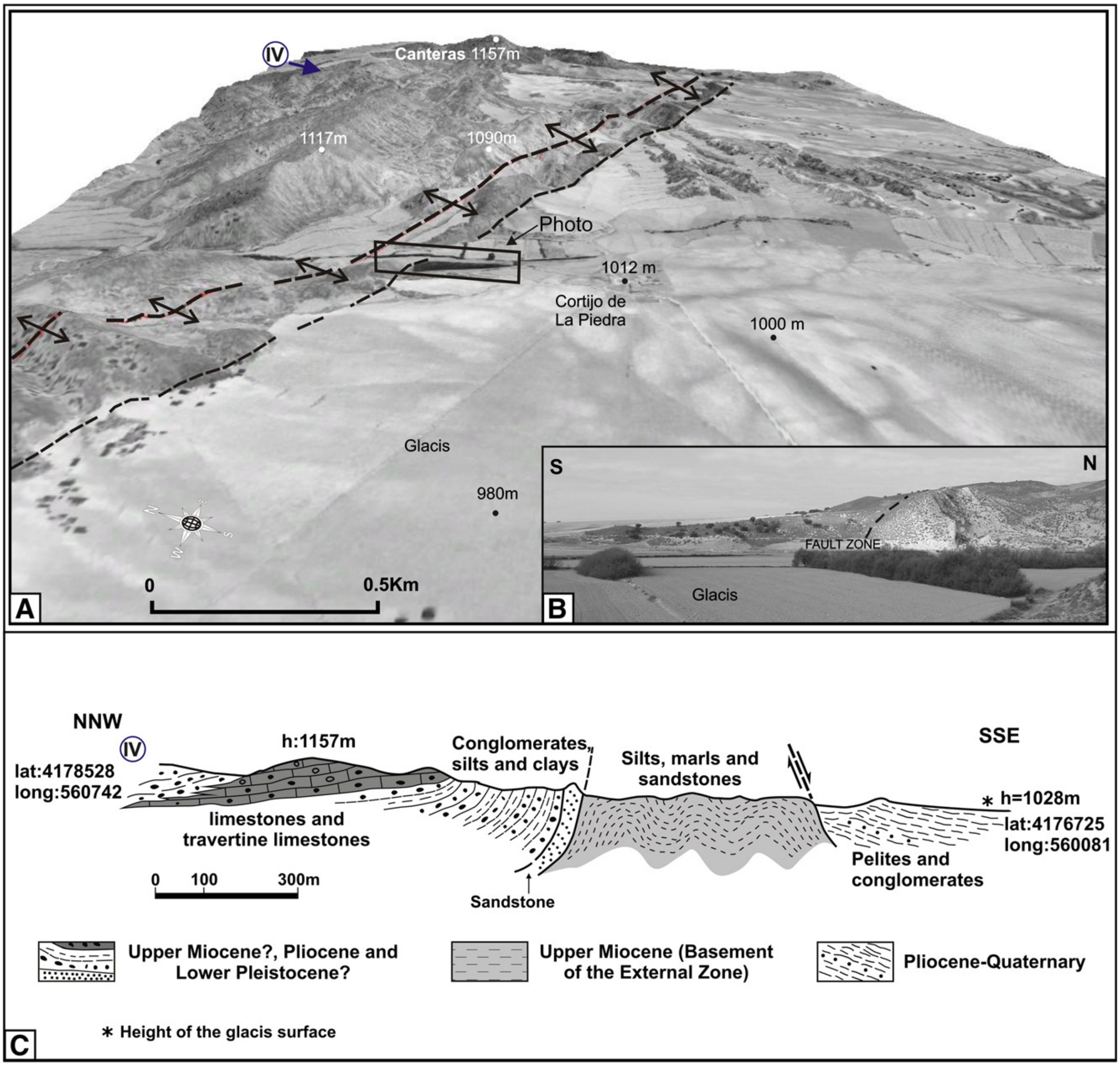

Fig. 5. A. DEM panoramic view of the Alfahuara southern limb. B. Panoramic view of the Alfahuara fold. C. Geological cross-section of the Alfahuara fold. Their locations are indicated in Fig. 1.

authors (Peña, 1985; Calvache and Viseras, 1997) used this age of around 100 ka to date the endhoreic–exorheic transitional period. The age of the glacis has also been recently proposed as 42 ka using a radiometric dating of a calcrete of edaphic origin formed on the top of the stratigraphic succession in the western part of the basin (Azañón et al., 2006; Pérez-Peña et al., 2009).

Taking into account: (1) new dating of the Solana del Zamborino site at 750 ka and the new estimate of 600 ka for the most recent endorheic materials discovered (Scott and Gibert, 2009); and (2) the age of exorheic sediments with results of 239 ka (Ortiz et al., 2000) and 205 ka (Díaz-Hernández and Juliá, 2006); the transition must have taken place during this period of time. This is in agreement with García-Tortosa et al. (2008) who proposed an age of around 400 ka. This age is based on the vertical displacement of the glacis by the Baza Fault and the average vertical slip rate of this active fault calculated by Alfaro et al. (2008).

After the endhoreic to exorheic transitional stage, deformation in the basin is recorded not only in the accumulated sediments, but also in the now inactive surface of the glacis. Considering the well-known pre-deformational geometry and estimated age of this paleosurface, we have undertaken a morphometric study to analyse the most recent deformation produced in the basin (from the latest middle Pleistocene to the present).

4. Methodology

In addition to detailed field work, previously published geological mapping has been revised. We also mapped the deformation structures using aerial photographs and satellite images. All this information has been integrated into the Geographic Information System (GIS). The preparation of this GIS, in addition to the geological and geomorphological data, includes digital orthographic images and high resolution DEM.

Quantitative analysis of the current morphology of the glacis has been carried out systematically for the whole basin. Anomalies of this surface were measured with respect to the original morphology which is considered to be pre-deformational.

Fig. 6. A. Panoramic view of the central and northern part of the Galera Fault zone showing the vertical displacement of the glacis. B and C. Panoramic view of several folds in the Galera sector.

In order to reconstruct the original morphology of the glacis (pre-deformational) different topographic profiles were prepared using GIS in areas where recent tectonic structures do not exist. In each of these profiles, which connect different borders of the basin, an envelope was traced that joins the preserved glacis surfaces. These envelopes represent the prolongation of the glacis surface, in the absence of erosion and deformation. This surface was reconstructed using a low degree polynomial function in order to extract the trends of the glacis; then, this envelope was translated to the maximum height of the glacis surface (García-Tortosa et al., 2008). In this way, the original morphology in the undeformed eroded sectors was reconstructed. These envelopes were then extrapolated to be compared with the deformed areas.

In order to detect anomalies in the glacis surface, topographic profiles were traced crossing the recognized tectonic structures in the basin. Following the same methodology as in the undeformed areas, we generated envelopes from well preserved glacis surfaces (e.g. P1 and P2 in Fig. 8). In this case, it was also possible to reconstruct the eroded parts. These envelopes of the current geometry of the glacis have enabled us to: (1) recognize glacis deformation, (2) identify which structures they produce, and (3) quantify the fault vertical slip and relative uplift folding rates.

Profiles were located where fault vertical slip and relative uplift folding rates were highest. It must be taken into account that in all the tectonic structures described, folds as well as faults, the greatest glacis displacement decreases toward their ends. On these ends (undeformed areas), the glacis has the same height at both sides of the structure.

In the study of the active faults, various profiles were generated in which the glacis envelope was represented on both sides of the fault. The glacis envelope in the foot wall generally coincides with the pre-deformational envelope. In the hanging wall, in places where erosion made it difficult to generate the envelope, we generated several envelopes assuming maximum and minimum erosion values. In this way minimum and maximum values of displacement were estimated as described in the Baza Fault (García-Tortosa et al., 2008). The difference in altitude between the intersections of both envelopes in the foot and hanging walls with the fault plane or its prolongation enabled us to estimate the vertical displacement. In the case of the folds, we estimated the differences between the crests and troughs of

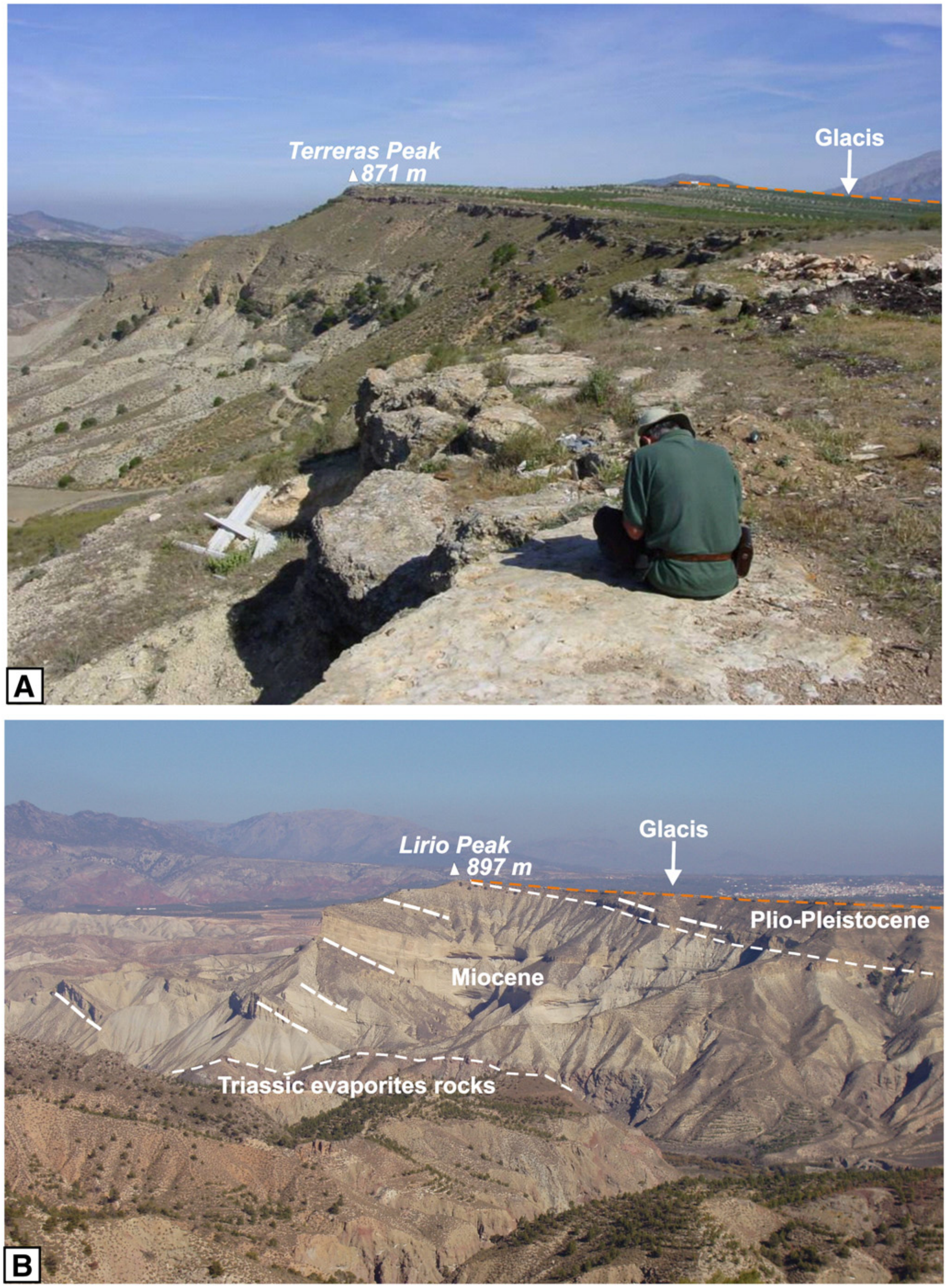

Fig. 7. Panoramic views of folded upper Miocene to Pleistocene rocks in the Guadiana Menor sector. A. Terreras Peak, eastern limb of an anticline where glacis is deformed. B. Lirio Peak, western limb of the NNE–SSW syncline. Note in the hinge zone of the fold the presence of Triassic evaporites and clays (red colour) of halokinetic origin.

the folded envelope with respect to its pre-deformational geometry in that sector.

5. Deformation of the glacis

From the profiles shown in Figs. 8, 9 and 10, compared to the information provided by several geological cross-sections (some of them are included in Figs. 2 to 5), we estimated the vertical displacement of the glacis. This deformation was caused by the main active faults and folds of the Guadix–Baza basin.

The displacement of the Baza Fault deduced in a narrow fault zone in its central part is 100 m (García-Tortosa et al., 2008) (Fig. 8). The Zamborino Fault (Fig. 8) caused a throw in the glacis of about 50 m, accumulated by several splays. Likewise, the Graena Fault caused an accumulated displacement of around 40 m. The Galera Fault caused an accumulated displacement of the glacis of 50 m in the central segment of the fault (Fig. 9).

The effects of the Alfahuara anticline on the glacis surface are difficult to estimate due to the proximity to the edge of the basin. Here, the glacis surface begins at the southern limb of the fold at a greater height than in other sectors of the basin. In this area it is not possible to distinguish between the slope increase caused by the edge effect and by folding. Taking into account that folds with a similar trend, situated immediately to the south in the Galera area, deform the glacis, we interpret that this slope is probably partially produced by the Alfahuara fold. As a pre-deformational envelope cannot be generated (between undeformed edges), the estimate of the uplift values produced by the fold is only qualitative.

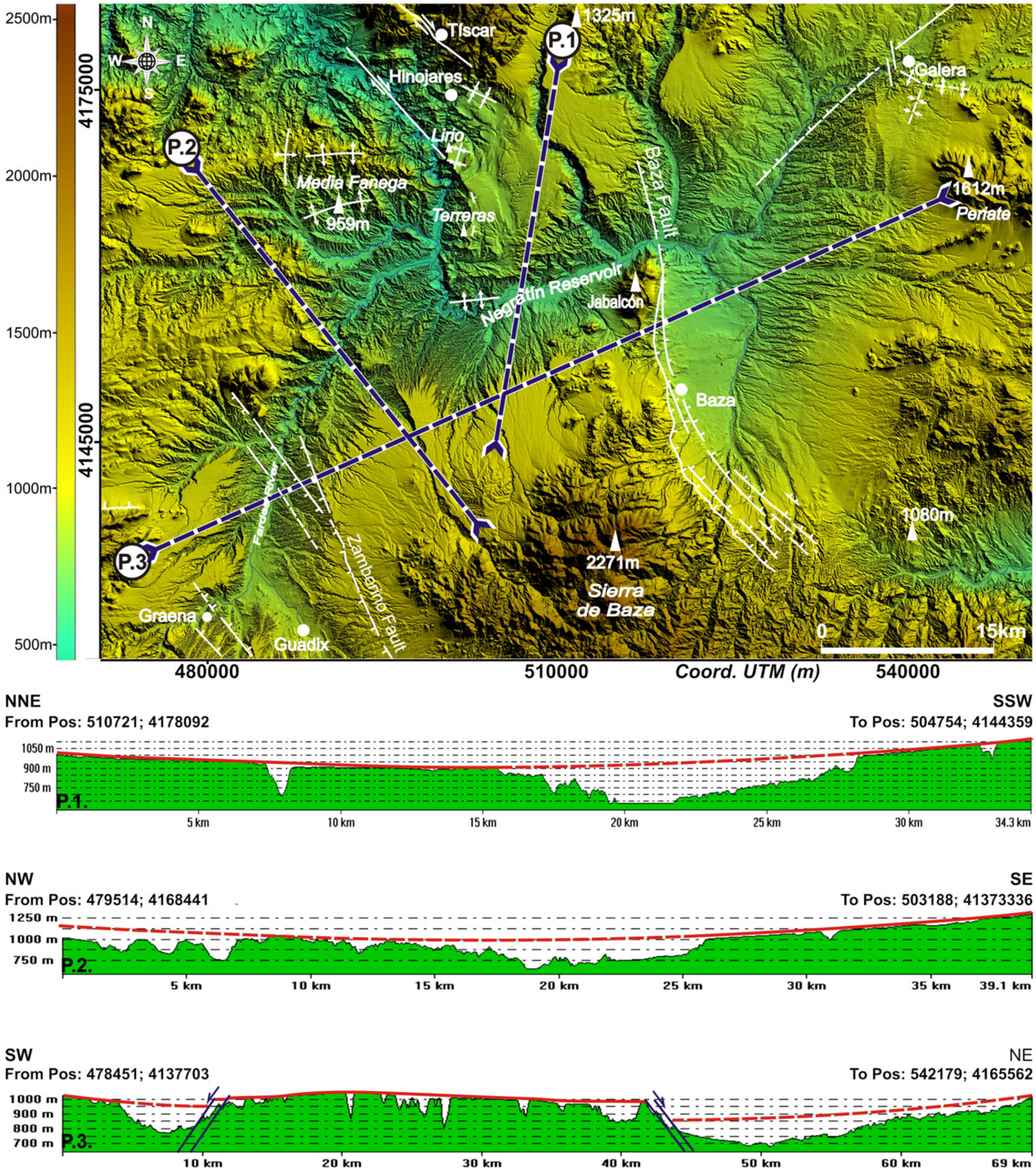

Fig. 8. DEM of the central zone of the basin and topographic profiles including the reconstruction of the glacis surface (envelope with red line). The position of the profiles is indicated in the DEM. P1: NNE–SSW topographic profile along a non deformed area. P2: Topographic profile in an area where glacis is eroded. The original glacis surface is reconstructed (see envelope with red dashed line) from the envelope obtained in the profile 1. P3: Topographic profile orthogonal to the Baza and Zamborino Faults. The reconstructed glacis surface shows a horst. Red-dashed line in the hanging wall of both faults is drawn taking into account the possible erosion of the original glacis surface.

In the Galera sector, the NNW–SSE profile (P5 in Fig. 9) shows a gently folded glacis. In this area, the glacis is displaced 30 m with respect to the pre-deformational geometry (dashed blue line). Pliocene and Pleistocene beds dip by up to 30° (Fig. 6), whilst the glacis surface is gently folded, which indicates that deformation has been occurring progressively over time since the Pliocene to the present.

In the Guadiana Menor sector, several NNE–SSW folds deform the glacis. The NW–SE profile (P6 in Fig. 10) shows a folded glacis displaced 35 m above the pre-deformational geometry (dashed blue line). The NE–SW profile (P7 in Fig. 10) shows the eastern limb of the Terreras fold (the western one is eroded by the Guadiana Menor River). Although the glacis is deformed, as shown in profile 7, it is not possible to quantify the uplift with respect to the unknown pre-deformational geometry at this sector. Even further to the north of these structures, the glacis is gently folded by the Hinojares syncline, but due to erosion its total vertical displacement cannot be calculated.

5.1. Vertical slip rates and folding rates

Taking into account the aforementioned vertical displacements of the glacis caused by several active faults and folds and the age of this

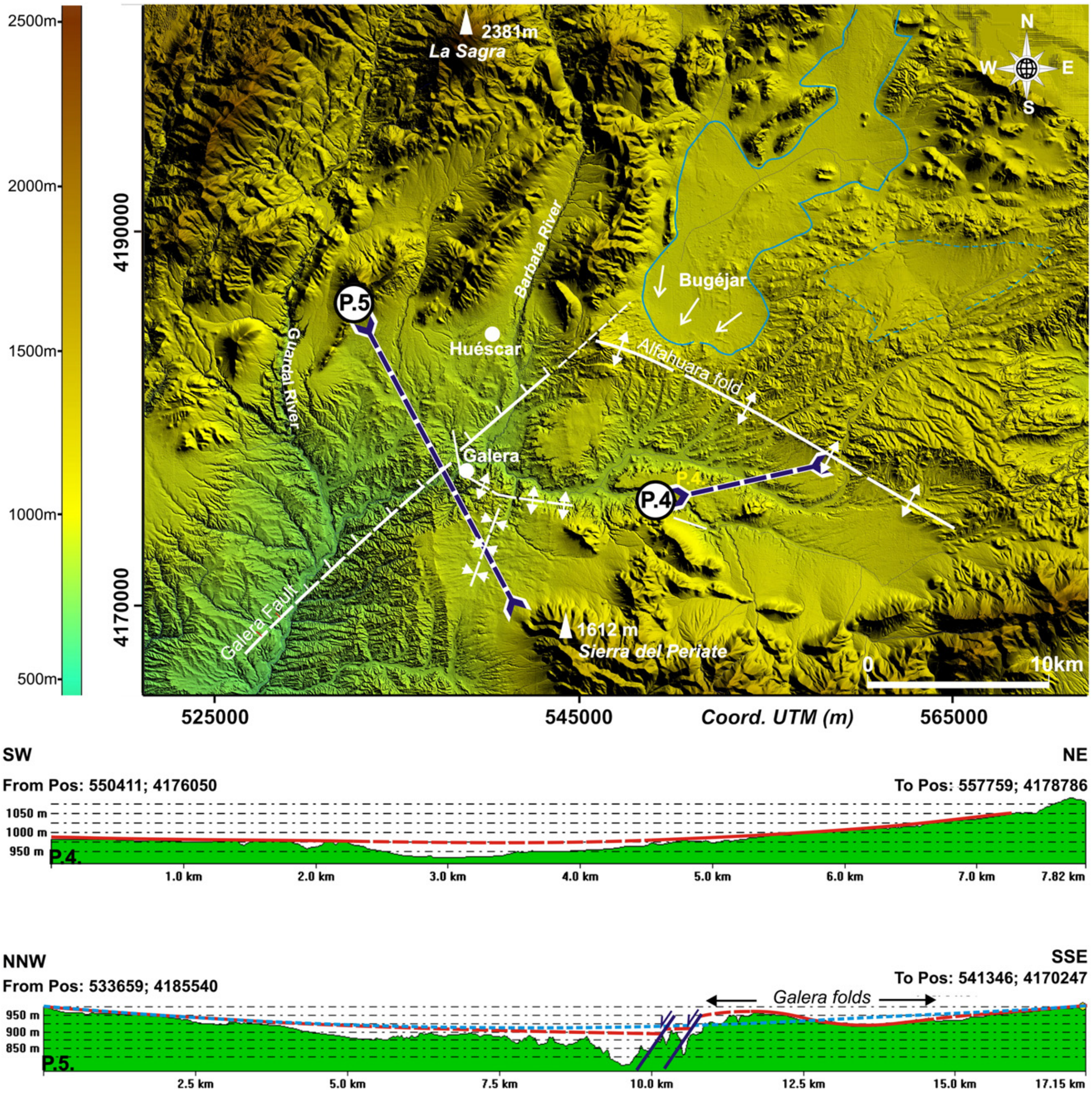

Fig. 9. DEM of the Galera and Alfahuara area in the eastern part of the basin, with location of two topographic profiles where glacis is deformed. Topographic profiles including the reconstruction of the deformed glacis surface (envelope with red-dashed line) and the possible reconstruction of the non-deformed glacis surface (blue-dashed line). P4: NE–SW profile of the SW limb of the Alfahuara fold. A steep slope is probably produced by the activity of this fold. P5. NW–SE profile across the Galera Fault. The red-dashed line corresponds to the glacis envelope in the eroded sectors in both walls of the Fault. The envelope of the foot wall also shows the folded glacis. The blue dashed line indicates the assumed undeformed glacis surface along this profile.

geomorphic surface, vertical slip rates of these faults as well as vertical folding rates were estimated.

Because several ages have been assigned to this geomorphic surface, a minimum and a maximum rate were calculated for each structure. The age range of the glacis varies between 600 ka, the age of the most recent endorheic sediments (Scott and Gibert, 2009), and the 205 ka age of the older exorheic sediments (Díaz-Hernández and Juliá, 2006).

The vertical slip rates of the main faults of the Guadix–Baza basin varies between 0.17 and 0.49 mm/year for the Baza Fault, 0.08 and 0.24 mm/year for the Zamborino and Galera Faults, and 0.07 and 0.19 mm/year for the Graena Fault.

In the Galera area, the 30 m of glacis displacement by folding, implies vertical folding rates varying between 0.05 and 0.15 mm/year. The vertical folding rates of the Lirio folds (Guadiana Menor River area), which caused a vertical displacement of 35 m, varies between 0.06 and 0.17 mm/year.

6. Discussion and conclusions

The Guadix–Baza basin is characterized by the coexistence of active compression and extension structures. Among these active structures, the normal faults at Baza, Zamborino and Graena, the left-lateral normal Galera Fault, the Galera folds and the Guadiana Menor folds dominate the glacis landscape. These faults, with associated seismicity, and folds deform the younger sediments, which fill the basin and are mid-Pleistocene in age. Although no regional stratigraphic markers exist from the mid-Pleistocene, a planar geomorphic

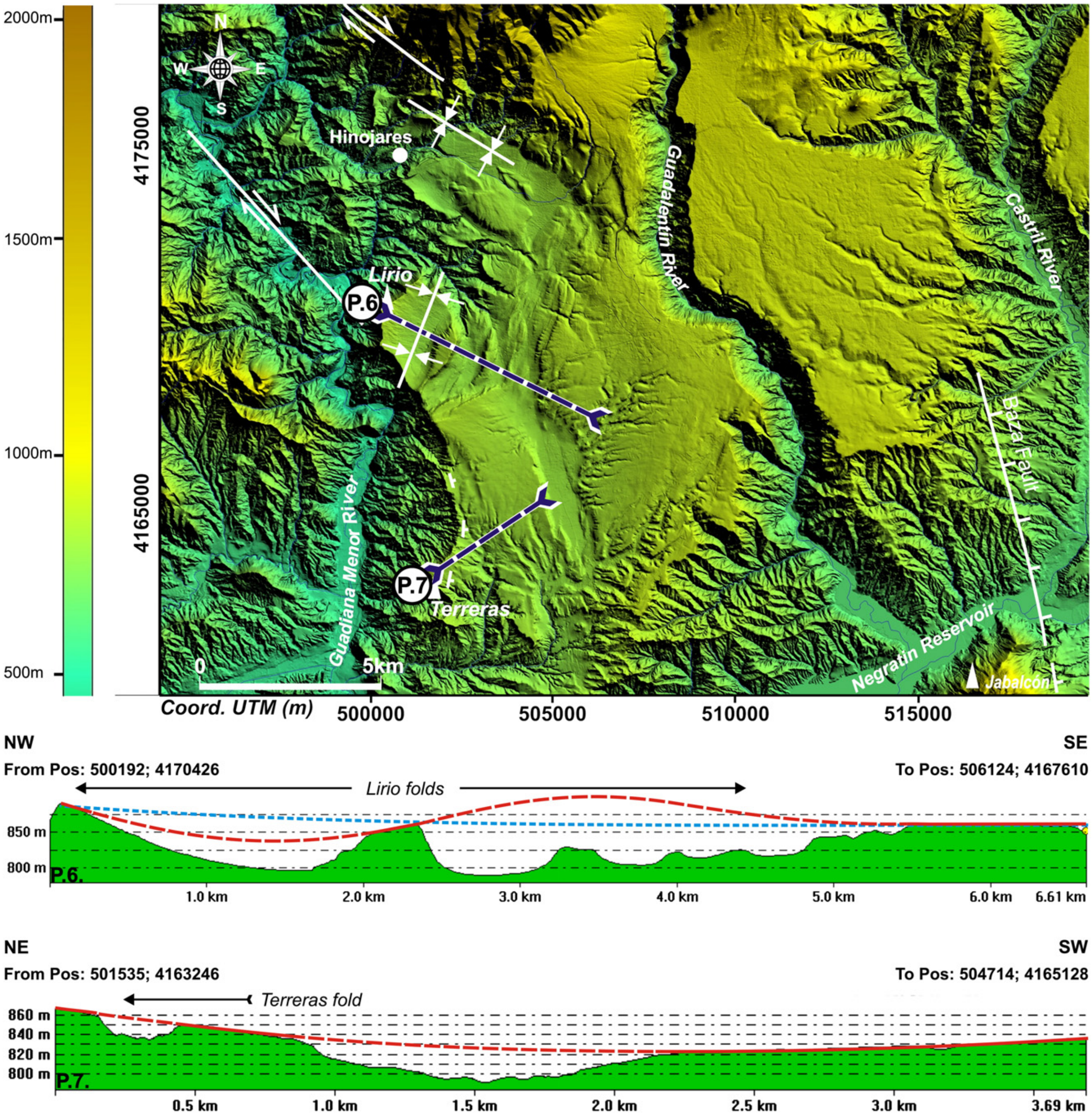

Fig. 10. DEM of the Guadiana Menor folded area with location of two topographic profiles where the glacis surface is folded. The red line corresponds to the deformed envelope, while the blue line corresponds to the assumed undeformed envelope. P6. NW–SE profile across the Lirio Peak syncline. P7. NE–SW profile across the Terreras Peak anticline.

marker has been used to study the more recent deformation of the basin. The glacis surface is eroded in some parts of the basin, especially in the central sector. Subsequently its morphometric analysis has not provided information on all the tectonic structures described in this field work. However, in those parts where it is preserved it is evident that some of these structures are still tectonically active.

The assumed age of this geomorphic marker is between 600 ka and 205 ka, according to Scott and Gibert (2009) and Díaz-Hernández and Juliá (2006), respectively. Younger ages proposed by Azañón et al. (2006) are discussed below.

The vertical slip rates estimated for the Baza Fault using this geomorphic marker, ranging from 0.17 to 0.49 mm/year, are in agreement with extension rates previously estimated by Alfaro et al. (2008) from an Upper Miocene stratigraphic marker, which varies between 0.11 and 0.33 mm/year. Future chronostratigraphic work will be very useful for estimating the age of the glacis more precisely and, consequently, to better constrain our proposed vertical slip rates.

The vertical slip rates obtained for the Zamborino Fault (0.08–0.24 mm/year) and the Graena Fault (0.07–0.19 mm/year) are slightly lower than those of the Baza Fault, suggesting a progressive westward decrease in slip rates.

The estimated rates in the Galera area are between 0.13 and 0.39 mm/year. Nevertheless, this value is the result of the combined activity of the Galera Fault (0.08–0.24 mm/year) and the Galera folds (0.05–0.15 mm/year).

In the case of the Guadiana Menor folds, we have calculated minimum values of around 0.06 and 0.17 mm/year. In this area, part of this vertical deformation could be caused by gravitational forces due to the presence of Triassic evaporites. In the folds that deform the glacis in the NW (Hinojares) and NE (Alfahuara) sectors, we are not able carry out the calculation as both are situated at the present margin of the basin. The present glacis slope is due to the combined effect of erosive-depositional processes and deformation, but the relative contribution is unknown.

The deduced vertical slip rates are of the same order of magnitude as those estimated by Gil et al. (2002) in the Granada basin, which is also located in the Central Betic Cordillera. These authors calculated a minimum extensional rate of 0.15–0.30 mm/year along a 15 km-long geological cross-section located in the NE part of the Granada basin, orthogonal to several active normal faults. In relation to vertical folding rates, Giménez et al. (2009), using a Pliocene stratigraphic marker and a high-precision nivelation profile obtain values varying between 0.1 and 0.2 mm/year in the Eastern Betic Cordillera. In addition, these values are also of the same order of magnitude as the uplift rates deduced in the Central Betic Cordillera from the Late Miocene to the present (Braga et al., 2003; Sanz de Galdeano and Alfaro, 2004). These studies indicate that the greatest uplift of the Betic Cordillera, of 0.5 mm/year, is located in Sierra Nevada, which is the southernmost basement of the Guadix–Baza basin. Nevertheless, these values disagree with those assigned to the Baza Fault by Pérez-Peña et al. (2009). These authors, based on a glacis age of 42 ka (sensu Azañón et al., 2006), obtained a higher Quaternary slip rate varying between 1.95 and 2.65 mm/year. These much higher rates disagree with the regional geodynamic setting characterized by low convergence (around 5 mm/year) between the African and Eurasian plates (DeMets et al., 1994) and with the low seismic activity of the region (Buforn et al., 1995; Peláez and López Casado, 2002).

However, ages of between 205 and 600 ka, as used in this work, fit better with those calculated previously by Alfaro et al. (2008) using the upper Miocene as a stratigraphic marker.

This study also provides evidence of the complex setting in the shallowest part of an orogen under compression like the Betic Cordillera, where extension and compression structures develop simultaneously in different nearby sectors. In general, at present the main regional driving mechanism is the NW–SE Eurasian–African plate convergence. In this setting, NW-SE trending compression and secondary NE-SW extension structures are expected. However, NE–SW oriented and unexpected normal faults, like the Galera Fault, may be a consequence of the shallow gravitational collapse of the thickened orogen, although future detailed studies of this fault are needed.

The NE–SW extension could also be another consequence of gravitational collapse. The detailed analysis developed in the study region provides evidence of high variability of vertical slip rates along the NE–SW orientation crossing the NW–SE fault set, with increasing values northeastwards from Graena to the Baza Fault. However, following northeastwards, in the same profile, the extensional rates become NE–SW shortening in the Alfahuara anticline.

The detailed analysis of the geometry of the Guadix–Baza basin glacis has been proven to be a suitable tool for studying active extensional and compressional deformation in large areas affected by folds and faults, even in the absence of recent sediments. This analysis contributes to location and classification of the regional tectonic structures according to their relative activity. The accuracy in the estimation of vertical slip and folding rates is strongly influenced by the precision of glacis dating.

Acknowledgements

The authors acknowledge the helpful comments by Klaus Reicherter and an anonymous referee which have improved the manuscript. This work has been financed through projects CGL2006-10202/BTE, CGL2007-60535/BTE, CSD2006-00041, CGL2009-07721/MEC and the Junta de Andalucia (Andalusian Autonomous Council) groups RNM217, 148 and 325.

References

Alfaro, P., Delgado, J., Sanz de Galdeano, C., Galindo-Zaldívar, J., García-Tortosa, F.J., López-Garrido, A.C., López-Casado, C., Marín, C., Gil, A., Borque, M.J., 2008. The Baza Fault: a major active extensional fault in the Central Betic Cordillera (South Spain). International Journal of Earth Sciences 97, 1353–1365.

Alfaro, P., Gibert, L., Moretti, M., García-Tortosa, F.J., Sanz de Galdeano, C., Galindo-Zaldívar, J., López-Garrido, A.C., 2010. The significance of giant seismites in the Plio-Pleistocene Baza paleolake (S Spain). Terra Nova 22, 172–179.

Azañón, J.M., Tuccimei, P., Azor, A., Sánchez-Almazo, I.M., Alonso-Zarza, A.M., Soligo, M., Pérez-Peña, J.V., 2006. Calcrete features and age estimates from U/Th dating: implications for the analysis of Quaternary erosion rates in the northern limb of the Sierra Nevada range (Betic Cordillera, Southeast Spain). In: Alonso-Zarza, A.M., Tanner, L.H. (Eds.), Paleoenvironmental Record and Applications of Calcretes and Palustrine Carbonates. Geological Society of America Special Paper, pp. 223–239.

Botella, M., Martínez, C., Cárdenas, F.J., 1985. Las industrias paleolíticas de Cueva Horá (Darro, Granada). Antropología y Paleoecología Humana 1, 59–74.

Braga, J.C., Martín Martín, J.M., Quesada, C., 2003. Patterns and average rates of late Neogene—recent uplift of the Betic Cordillera, SE Spain. Geomorphology 50, 3–26.

Buforn, E., Sanz de Galdeano, C., Udías, A., 1995. Seismotectonics of the Ibero-Maghrebian region. Tectonophysics 248, 247–261.

Burbank, D.W., Anderson, R.S., 2001. Tectonic Geomorphology. Blackwell, Massachusetts.

Calvache, M.L., Viseras, C., 1997. Long-term control mechanisms of stream piracy processes in southeastern Spain. Earth Surface Processes and Landforms 22, 93–105.

DeMets, C., Gordon, R.G., Argus, D.F., Stein, S., 1994. Effect of recent revisions to the geomagnetic reversal time scale on estimates of current plate motions. Geophysical Research Letters 21, 2191–2194.

Díaz-Hernández, J.L., Juliá, R., 2006. Geochronological position of badlands and geomorphological patterns in the Guadix–Baza basin (SE Spain). Quaternary Research 65, 467–477.

Estévez, A., López-Garrido, A.C., Sanz de Galdeano, C., 1978. Estudio de las deformaciones recientes en el sector del Negratín (Depresión de Guadix Baza). Comisión Nacional para el Proyecto Geodinámico. Reunión sobre la Geodinámica de la Cordillera Bética y Mar de Alborán. Universidad de Granada, pp. 165–192.

Filocamo, F., Romano, P., Di Donato, V., Esposito, P., Mattei, M., Porreca, M., Robustelli, G., Russo Ermolli, E., 2009. Geomorphology and tectonics of uplifted coasts: new chronostratigraphical constraints for the Quaternary evolution of Tyrrhenian North Calabria (southern Italy). Geomorphology 105, 334–354.

Galindo-Zaldívar, J., Gil, A.J., Borque, M.J., González-Lodeiro, F., Jabaloy, A., Marín-Lechado, C., Ruano, P., Sanz de Galdeano, C., 2003. Active faulting in the internal zones of the central Betic Cordilleras (SE, Spain). Journal of Geodynamics 36, 239–250.

García-Tortosa, F.J., Alfaro, P., Galindo Zaldívar, J., Gibert, L., López Garrido, A.C., Sanz de Galdeano, C., Ureña, M., 2008. Geomorphologic evidence of the active Baza Fault (Betic Cordillera, south Spain). Geomorphology 97, 374–391.

Gibert, L., 2006. Analisis de facies y magnetostratigrafia de la cuenca de Baza. Ph.D. Thesis, Univ. Politècnica de Catalunya, Manresa, Spain.

Gibert, L., Sanz de Galdeano, C., Alfaro, P., Scott, G.R., López-Garrido, A.C., 2005. Seismic-induced Pleistocene landslides in deltaic deposits of the Baza basin (SE Spain). Sedimentary Geology 179, 279–294.

Gibert, L., Ortí, F., Rosell, L., 2007. Plio-Pleistocene lacustrine evaporites of the Baza Basin (Betic Chain, SE Spain). Sedimentary Geology 200, 89–116.

Gil, A.J., Rodríguez-Caderot, G., Lacy, M.C., Ruiz, A.M., Sanz de Galdeano, C., Alfaro, P., 2002. Establishment of a non-permanent GPS network to monitor the recent deformation in the Granada Basin (Betic Cordillera, Southern Spain). Studia Geophysica et Geodaetica 46, 395–410.

Giménez, J., Borque, M.J., Gil, A., Alfaro, P., Estévez, A., Suriñach, E., 2009. Comparison of long-term and short-term uplift rates along an active blind reverse fault zone (Bajo Segura, SE Spain). Studia Geophysica et Geodaetica 53, 81–98.

Goy, J.L., Zazo, C., 1986. Synthesis of the Quaternary in the Almería littoral. Neotectonic activity and its morphologic features, Western Betics, Spain. Tectonophysics 130, 259–270.

Goy, J.L., Zazo, C., Bardají, T., Somoza, L., Causse, C., Hillaire-Marcel, C., 1993. Eléments d'une chronostratigraphie du Tyrrhénien des régions d'Alicante-Murcie, Sud-Est de l'Espagne. Geodinamica Acta 6-2, 103–119.

Gutiérrez, F., Gutiérrez, M., Gracia, F.J., McCalpin, J.P., Lucha, P., Guerrero, J., 2008. Plio-Quaternary extensional seismotectonics and drainage network development in the central sector of the Iberian Chain (NE Spain). Geomorphology 102, 21–42.

Hall, S.R., Farber, D.L., Audin, L., Finkel, R.C., Mériaux, S., 2008. Geochronology of pediment surfaces in southern Peru: implications for Quaternary deformation of the Andean forearc. Tectonophysics 459, 186–205.

Hetzel, R., Niedermann, S., Tao, M.X., Kubik, P.W., Ivy-Ochs, S., Gao, B., Strecker, M.R., 2002. Low slip rates and long-term preservation of geomorphic features in Central Asia. Nature 417, 428–432.

Hetzel, R., Tao, M.X., Stokes, S., Niedermann, S., Ivy-Ochs, S., Gao, B., Strecker, M.R., Kubik, P.W., 2004a. Late Pleistocene//Holocene slip rate of the Zhangye thrust (Qilian Shan, China) and implications for the active growth of the northeastern Tibetan Plateau. Tectonics 23. doi:10.1029/2004TC001653.

Hetzel, R., Tao, M.X., Niedermann, S., Strecker, M.R., Ivy-Ochs, S., Kubik, P.W., Gao, B., 2004b. Implications of the fault scaling law for the growth of topography: mountain ranges in the broken foreland of NE Tibet. Terra Nova 16, 157–162.

Keller, E.A., Pinter, N., 1996. Active Tectonics (Earthquakes, Uplift and Landscape). Prentice-Hall Inc, New Jersey.

López-Garrido, A.C., Vera, J.A., 1974. Diapirismo reciente en la depresión de Guadix–Baza (Sector del Negretín). Estudios Geológicos 30, 611–618.

López-Casado, C., Molina, S., Giner, J.J., Delgado, J., 2000. Magnitude-intensity relationships in the Ibero-Magrebhian Region. Natural Hazards 22, 269–294.

Martínez-Solares, J.M., Mezcua, J., 2002. Catálogo sıísmico de la Península Ibérica (880 AC-1900). Instituto Geográfico Nacional, Monografía nº 18 , Madrid Spain, pp 1–254.

Mayer, L., 1986. Tectonic geomorphology of escarpments and mountain fronts. In: Wallace, R.E. (Ed.), Active Tectonics. Studies in Geophysics. National Academy Press, Washington, DC, pp. 125–135.

Ortiz, J.E., Torres, T., Llamas, J.F., Canoira, L., García-Alonso, P., García de la Morena, M.A., Lucini, M., 2000. Dataciones de algunos yacimientos paleontológicos de la cuenca de Guadix–Baza (sector de Cúllar-Baza, Granada, España) y primera estimación de edad de la apertura de la cuenca mediante el método de racemización de aminoácidos. Geogaceta 28, 109–112.

Peláez, J.A., López Casado, C., 2002. Seismic hazard estimate at the Iberian Peninsula. Pure and Applied Geophysics 159, 2699–2713.

Peláez, J.A., Sanz de Galdeano, C., López Casado, C., 2007. Determinación preliminar del potencial sísmico de la Cuenca de Guadix–Baza (Granada). 3er Congreso Nacional de Ingeniería Sísmica. Girona (Spain) 265–273.

Peña, J.A., 1985. La depresión de Guadix-Baza. Estudios Geológicos 41, 33–46.

Pérez-Peña, J.A., Azañón, J.M., Azor, A., Tuccimei, P., Della Seta, M., Soligo, M., 2009. Quaternary landscape evolution and erosion rates for an intramontane Neogene basin (Guadix–Baza basin, SE Spain). Geomorphology 106, 206–218.

Ramírez, M.T., 1999. Geomorphic assessment of active tectonics in the Acambay Graben, Mexican volcanic belt. Earth Surface Processes and Landforms 23, 317–332.

Sanz de Galdeano, C., 1990. Geologic evolution of the Betic Cordilleras in the Western Mediterranean, Miocene to the present. Tectonophysics 172, 107–119.

Sanz de Galdeano, C., Alfaro, P., 2004. Tectonic significance of the present relief of the Betic Cordillera. Geomorphology 63, 175–190.

Schumm, S.A., Dumont, J.E., Holbrook, J.M., 2000. Active Tectonics and Alluvial Rivers. Cambridge University Press, UK.

Scott, G., Gibert, L., 2009. The oldest hand-axes in Europe. Nature 461, 82–85.

Silva, P.G., 1994. Evolución Geodinámica de la Depresión del Guadalentín desde el Mioceno Superior hasta la actualidad: Neotectónica y Geomorfología. Ph.D. Thesis, UCM, Madrid, Spain.

Silva, P., Goy, J., Zazo, C., Bardaji, T., 2003. Fault-generated mountain fronts in southeast Spain: geomorphologic assessment of tectonic and seismic activity. Geomorphology 50, 203–225.

Vera, J.A., 1970. Estudio estratigráfico de la depresión de Guadix–Baza. Boletín Geologico y Minero 91, 429–462.

Viseras, C.A., 1991. Estratigrafía y sedimentología del relleno aluvial de la cuenca de Guadix (Cordilleras Béticas). Ph.D. Thesis, Univ. Granada, Spain.

Yeats, R.S., Sieh, K., Allen, C.R., 1997. The Geology of Earthquakes. Oxford University Press, Oxford, UK.

Zazo, C., Goy, J.L., Hillaire-Marcel, C., González-Delgado, A., Dabrio, C.J., Soler, V., Bardají, T., Gillot, P.Y., Silva, P.G., González-Hernández, F.M., Lario, J., 2000. Raised marine terraces as proxies for sea-level changes and sea-surface conditions (Atlantic–Mediteranean, Spain). In: Schnak, E.J., Murray-Wallace, C.V. (Eds.), Coastal Interactions during Sea-Level Highstands. Patagonia 2000—International Conference, International Geological Correlation Programme-Project 437, pp. 87–89.